

Full-system laboratory testing of the F/15 deformable secondary mirror for the new MMT adaptive optics system

P.C. McGuire^a, M. Lloyd-Hart^a, J.R.P. Angel^a, G.Z. Angeli^a, R.L. Johnson^a,
B.C. Fitz-Patrick^a, W.B. Davison^a, R.J. Sarlot^a, C.J. Bresloff^a, J.M. Hughes^a, S.M. Miller^a,
P. Schaller^a, F.P. Wildi^a, M.A. Kenworthy^a, R.M. Cordova^a, M.L. Rademacher^a,
M.H. Rascon^a, J.H. Burge^b, B.L. Stamper^b, C. Zhao^b, P. Salinari^c, C. Del Vecchio^c,
A. Riccardi^c, G. Brusa^c, R. Biasi^d, M. Andrighettoni^d, D. Gallieni^e, C. Franchini^f,
D.G. Sandler^g, T.K. Barrett^g

^aCenter for Astronomical Adaptive Optics, Steward Observatory,
University of Arizona, Tucson, AZ 85721

^bOptical Sciences Center, University of Arizona, Tucson, AZ 85721

^cOsservatorio Astrofisico di Arcetri, Largo Enrico Fermi 5, 50125 Firenze, ITALY

^dMicrogate S.r.l., Via Valdagno 4, I-39100 Bolzano, ITALY

^eADS Italia S.r.l., Corso Promessi Sposi 23/D, 22053 Lecco, ITALY

^fMedia Lario S.r.l. Località Pascolo, Bosisio Parini,
I-23842 Lecco, ITALY

^gTrex Enterprises, 10455 Pacific Center Court, San Diego, CA 92121

ABSTRACT

We will present a system to perform closed-loop optical tests of the 64 cm diameter, 336 actuator adaptive secondary made at the Steward Observatory Mirror Laboratory. Testing will include Shack-Hartmann wavefront sensing and modal correction of static and dynamic aberrated wavefronts. The test optical system (called the ‘Shimmulator’) is designed so that experiments can be made with both the focal plane instrument and secondary installed in their normal configuration at the MMT, or with the same 9 m spacing in a laboratory test tower. The convex secondary will be illuminated at normal incidence through two 70 cm diameter lenses mounted just below. The artificial, aberrated star is projected from near the wavefront sensor in the Cassegrain focus assembly. Computer generated holograms correct for spherical aberration in the relay optics at the test wavelengths of 0.594 and 1.5 μm . Atmospheric turbulence is reproduced by two spinning transmission plates imprinted with Kolmogorov turbulence. The Shimmulator will give us the opportunity to test fully the adaptive optics system before installation at the new MMT, hence saving much precious telescope time.

Keywords: MMT, Shimmulator, Adaptive Secondary

1. INTRODUCTION

We are nearing the end of the construction phase of the adaptive optics (AO) system for the new 6.5 meter Multiple Mirror Telescope (MMT). The MMT AO system will feature a 0.64 meter diameter 1.6 mm thick deformable convex secondary mirror with 336 voice coil electromagnetic actuators with an update rate of 1 kHz and a maximum stroke above 10 μm .¹ We expect to finish the electromechanical integration of the adaptive secondary in September 1999, and hope to have a fully operational natural guidestar adaptive optics system working at the MMT in early 2000.

Between the time of secondary delivery and MMT AO system first light, we will optically integrate the adaptive secondary into a test optics system at the Steward Observatory Mirror Laboratory, and then proceed to perform closed-loop testing of the full AO system. Since the test optics system has rotating turbulence plates, it can effectively simulate a telescope that observes stars through a shimmering atmosphere, so henceforth the MMT AO test optics

Other author information:

EMAIL:mcguire@as.arizona.edu; Telephone:(520)621-7870

system will be known as the ‘Shimmulator’.² We have recently completed the Shimmulator construction phase and are in the middle of the alignment phase. Our main reason for building the Shimmulator is to maximize the quantity and quality of high-resolution astronomical observing time with the MMT AO system. Without the Shimmulator and its optics to test a *convex* deformable secondary, we would be only able to test the MMT AO system with real starlight, and hence much valuable observing time (when we should be doing astronomy) would be lost. We are also building two more versions of the Shimmulator, one for off-telescope testing of the AO system on the mountain, and one for on-telescope, off-sky testing of the AO system.

Herein, we briefly review the key components of the new MMT’s AO system, give a systems-level description of the major components of the Shimmulator, and describe the important Shimmulator tests of the MMT AO system.

2. THE MMT ADAPTIVE OPTICS SYSTEM

2.1. Adaptive Optics with a Deformable Secondary Mirror

Our Italian collaborators (coordinated by Media Lario) are building the actuators and control electronics for our adaptive secondary mirror, and they will soon integrate the actuators and controls with the Arizona-built thin convex Zerodur glass shell and thick Ultra-Low Expansion (ULE) glass reference plate.¹ Brusa *et al.*³ made two key innovations which make the control of the large, thin, floppy mirror possible. First, they found if the gap between the thin shell and the reference plate was made small enough ($40\ \mu\text{m}$), then the thin layer of air in the gap effectively dampened all the troubling resonances in the mirror below 1 kHz. Second, if they implemented ‘feed-forward’ control of the mirror, then they avoided the slow response-time of the Proportional-Integral-Derivative (PID) control loop to high-stress, high-order modes, and hence regain 1kHz high-order control of the mirror. Feed-forward control consists of calculating the final-state forces of all the actuators for the required set of actuator positions, and then ‘instantly’ applying all these forces simultaneously in open-loop. PID closed-loop control of the mirror would clean-up the slight actuator errors at a much faster update rate.

2.2. Wavefront Sensor Camera and Wavefront Computer

We have built a Shack-Hartmann wavefront sensor (WFS) camera with a 12×12 array of subapertures, optimized for the MMT AO system.⁴ Our WFS camera has the 80×80 frame-transfer four-amplifier CCD39A from EEV, a permanently attached lenslet array from AOA, and a GenII Leach/SDSU CCD VME-based controller operating at a 1kHz frame rate. The compact WFS dewar is on a rotary stage that maintains the registration of the camera’s subapertures with the actuators behind the secondary mirror. Otherwise, without the rotary stage, the continual derotation of the focal-plane instrument on the Alt-Az telescope mount during a long observation would cause actuator-WFS misregistration and make AO impossible. The WFS has low noise (3.5–4.0 electrons/read) and low dark current (~ 1 electron/millisecond). The electronic cross-talk between CCD pixels is tolerably low, so that the WFS noise sensitivity (~ 0.7) is near minimal (0.5), and hence we can tolerate the dimmest possible guidestars. The WFS has been tested in closed-loop mode in our bench-top 37 actuator AO system,⁵ and we hope to soon demonstrate closed-loop 37 actuator correction with full dynamic turbulence created by two counter-rotating turbulence plates.

Trex Enterprises has built and recently delivered the real-time wavefront computer, which operates in a VME bus system, acquires data from the WFS, and computes the actuator commands to deform the secondary mirror. The wavefront computer passed our delivery requirements of taking simulated WFS images and calculating the correct actuator commands at 1kHz. The servo delay of 0.111 milliseconds is a fraction of the WFS integration time, and more than half of this delay is due to the latency of the matrix multiply operation, and maybe one-third of this delay is due to communication delay between the wavefront computer and the secondary. We will integrate the wavefront computer with the adaptive secondary after the secondary is delivered in September.

2.3. The Infrared Science Instruments

Don McCarthy’s team is building a custom near-infrared camera and spectrograph⁶ (ARIES) to complement the MMT AO system. The ARIES instrument will be bolted to a mating flange beneath the WFS Top Box, and the entrance window to the camera will be an infrared-transmitting and visible-light reflecting dichroic beam splitter. Therefore, since the secondary is the adaptive element of our system, the ARIES instrument will only see 2 warm surfaces (the primary mirror and the secondary mirror). Infrared astronomers using our adaptive secondary AO system with ARIES will avoid the contaminating thermal background of the 6–8 additional warm surfaces found in standard AO systems without adaptive secondaries. Hence, they can finish higher quality images or spectra in as

little as one-fifth the exposure time as infrared astronomers with standard AO.⁷ We are also planning to integrate an existing near-infrared camera (FSPEC)⁸ and an existing mid-infrared camera (MIRAC)⁹ into the MMT AO Top Box, so that these instruments can take full advantage of AO with minimal thermal background.

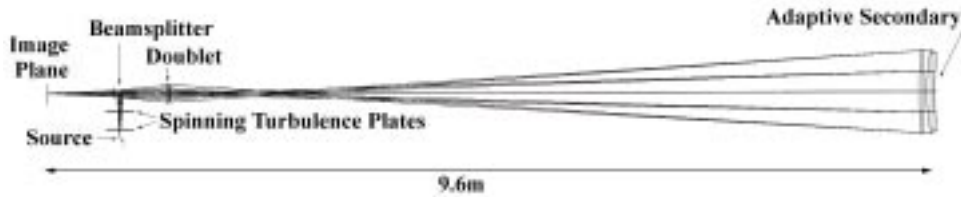


Figure 1. Shimmulator optical design.

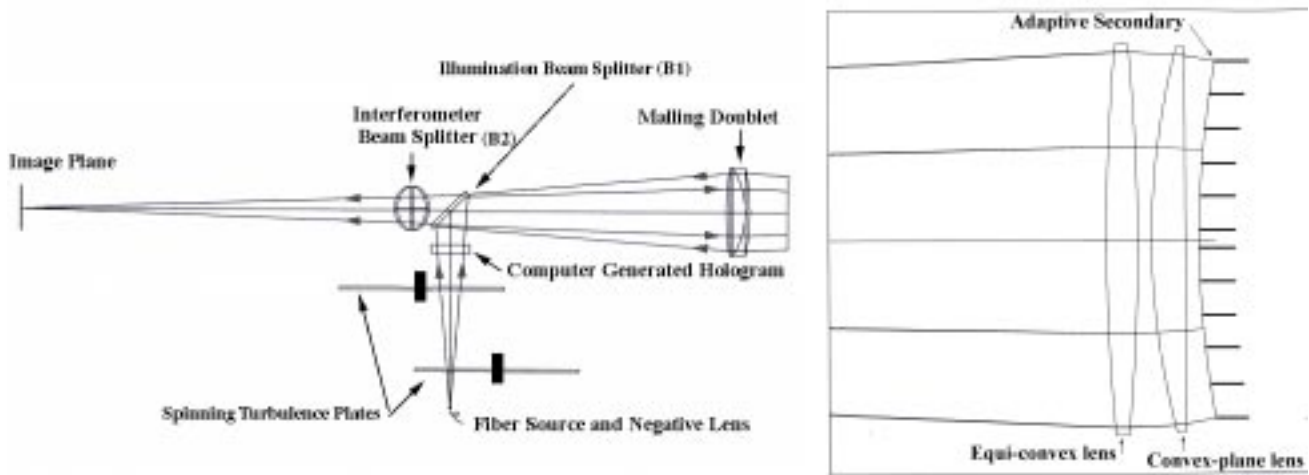


Figure 2. Diagrams of Shimmulator small optics (left) and large optics (right).

3. SHIMMULATOR OPTICAL AND MECHANICAL DESIGN AND IMPLEMENTATION

The MMT has a 9 meter back focal distance from the secondary, and the adaptive F/15 secondary has a convex shape. Therefore, in order to test the adaptive secondary optically in closed-loop in the presence of simulated turbulence, we needed to design and construct a tower (see Figs. 1-3) that supports not only the secondary, but also two large 0.70 meter diameter reimaging lenses (manufactured at the Steward Observatory Mirror Lab) and two large folding flat mirrors. The reimaging lenses serve to maintain the F/15 beam from the secondary, and they also ensure that the actuators have the same mapping in the Shimmulator as for real starlight (see Fig. 5). We designed the tower so that it could test our entire adaptive optics system, not just the secondary, so the tower also needed to support the Top Box, which may weigh up to 2500 pounds, as well as ARIES, which may weigh up to 500 pounds. The Top Box contains the wavefront sensor and its associated optics, and it serves as the telescope mating support structure for the infrared science instrument (e.g. ARIES, MIRAC or FSPEC). An air suspension system isolates the whole 8 ton tower from building vibrations at its location in the Mirror Lab.

The infrared ($1.55 \mu\text{m}$) and visible ($0.594 \mu\text{m}$) sources of the Shimmulator test light are mounted as a pair of fibers glued together nearly co-axially on a platform within the Top Box. This platform also supports a computer generated hologram (CGH).² The CGH adjusts (or predistorts) the infrared and visible wavefronts to correct for the 4000 waves of spherical aberration introduced by the large spherical lenses. The CGH also projects alignment markings to focus on-axis at several different crucial positions within the optical train (see Fig. 6). The CGH was manufactured by the Russian Academy of Sciences, Siberian Group. In the diverging light between the sources and the CGH, we will place two counter-rotating plates with imprinted turbulence (shown in Fig. 7) in order to

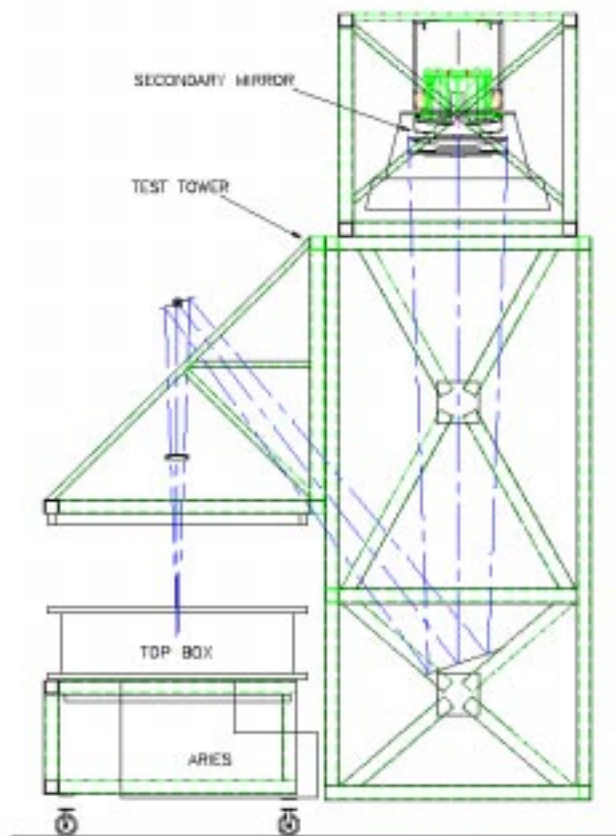


Figure 3. Shimmulator mechanical design, showing the large fold flats and the unmounted Top Box on its handling cart. The Top Box is normally raised from its handling cart and mounted to the dummy rotator ring just below the small doublet.

simulate the shimmering atmosphere.^{5,10,11} We will be able to control the effective spatial coherence length r_0 of the turbulence from each plate by changing the plates' distances from the sources. In addition, we can vary the effective wind speed corresponding to each plate from 0 to 50 m/s by controlling the speed of the the motors that rotate the plates. Note that this includes the case of static turbulence, which will be an indispensable diagnostic tool in the Shimmulator. After the CGH in the Shimmulator optical train (see Fig. 2, a beam splitter (B1) reflects the test light up through a small doublet (custom manufactured by TORC), onto the fold flats, through the two large lenses, off the secondary, back through the same optical system, and then back through the same beam splitter (see Fig. 1).

After the first beam splitter, a second beam splitter (B2, which is clocked at 90 degrees relative to the first beam splitter) reflects half the light to a diagnostic interferometer.^{12,13} The interferometer serves to monitor the quality of the optics without turbulence, and will also allow us to measure static turbulence at high spatial resolution, with and without correction by the adaptive secondary. At a beam splitter in the interferometer, the test beam from the Shimmulator interferes with a reference beam which is fiber-fed from the same laser that feeds the Shimmulator CGH source optics, and a Pulnix camera records the resulting interferogram. Durango software captures the interferograms and also controls a piezoelectric phase shifter in the laser source optics so we can reconstruct phasemaps from the observed fringes with great ease.

After passing through the second beam splitter (B2), the light is split again by the dichroic mirror that serves as the entrance window to ARIES, sending infrared light into the IR camera and reflecting visible light back up into the Top Box, through a third beam splitter. The third beam splitter sends half the visible light into a wide-field visible science and guidestar finding camera, and the other half off of two off-axis parabolas¹⁴(manufactured by Optical

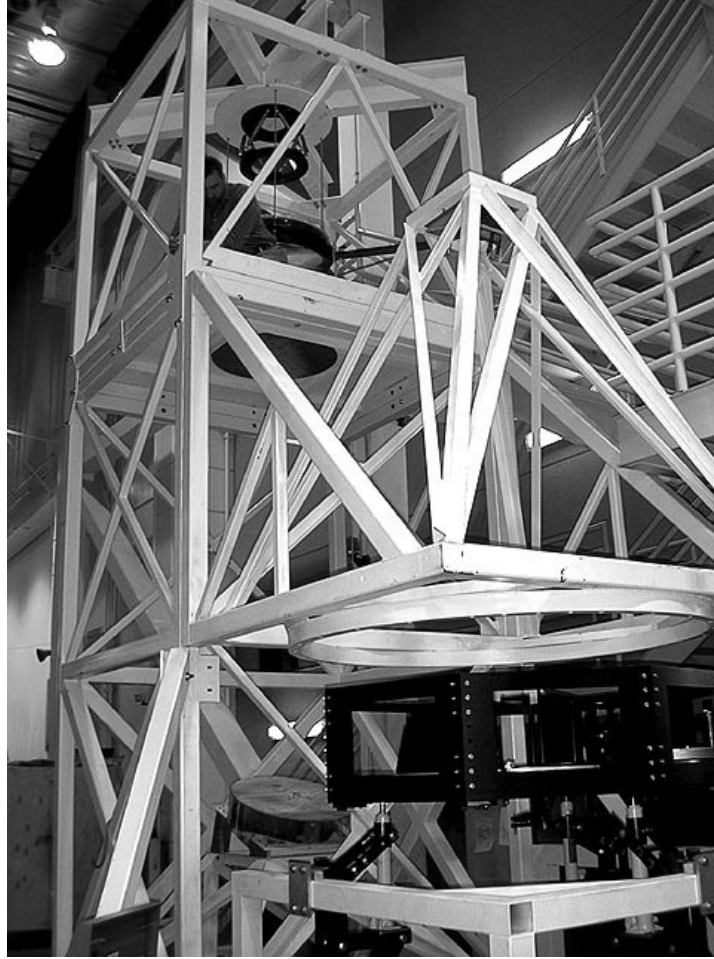


Figure 4. View of the as-built Shimmutator the Steward Observatory Mirror Laboratory, showing the covered large fold flat in the lower left, the unmounted & now-populated Top Box in the lower right, and our Principal Mechanical Engineer (B.F.) on the platform with the large lenses support structure. The Dummy Secondary has been added since this picture was taken, as shown in Fig. 8, to the dummy hexapod which is shown above the large lens cell at the top of the tower.

Surfaces Ltd, United Kingdom), and into the wavefront sensor camera. In initial Shimmutator tests, the ARIES dichroic mirror will be replaced by an 80% reflective beam splitter, the wide-field science camera will be replaced by a video rate Pulnix camera, and the ARIES infrared instrument will be replaced by a long-exposure visible science camera, but we should soon thereafter be able to put the existing ARIES predecessor, PISCES, at the infrared focus for infrared imaging tests in the Shimmutator.

The alignment of the whole Shimmutator and Top Box is a complex task, as we need to align some of the optical components (e.g. small doublet) to within $50 \mu\text{m}$ centration and spacing. We need to achieve these tolerances ‘mechanically’, without optical feedback from light reflected off of the secondary. We cannot rely on such optical feedback because the secondary is floppy and deformable and we do not know its initial shape. We must align the Shimmutator mechanically, test the Shimmutator optically with a dummy solid thick spherical secondary, install the deformable spherical secondary mirror, and then tune up the actuators to minimize the aberration, in that order.

Since February 1999, we have constructed and integrated the Shimmutator tower and optics (see Figs. 4 and 8). We have aligned the large optics (large lenses, small doublet, and large fold mirrors). We are using a Brunson alignment and auto-reflection telescope to determine the optical axis to within $50 \mu\text{m}$ at the small doublet and 1 mm at the large lenses, and a theodolite to measure the angular size of the large lenses and hence the distance between the large lenses and the small doublet to 1 mm accuracy over a 9 meter path length. We have run light through

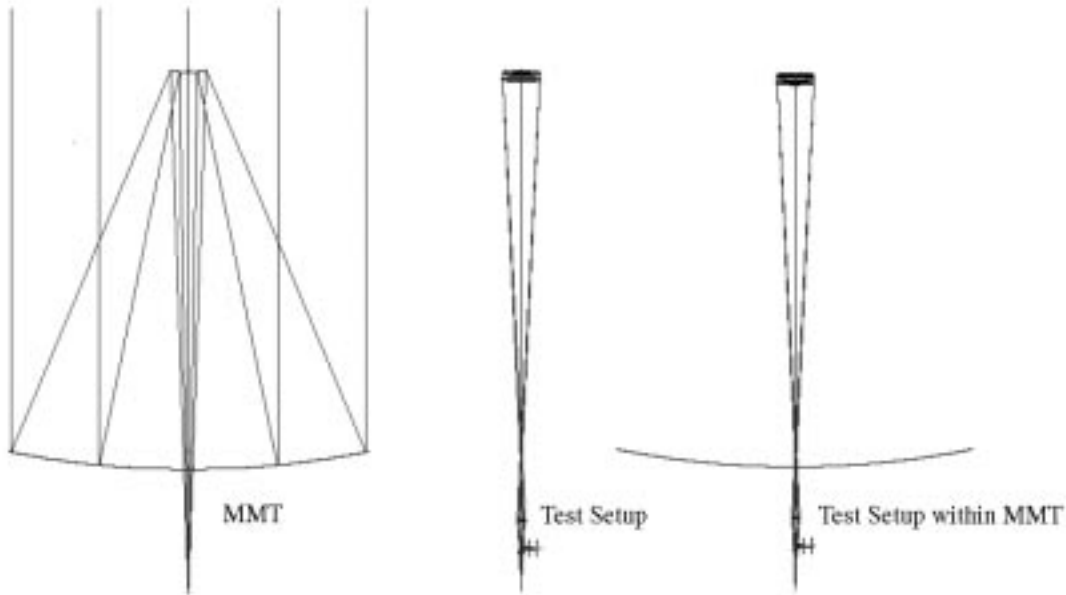


Figure 5. Diagram of mapping, showing the rays of light for the Cassegrain MMT on the left, for the Shimmulator without fold-flats in the center, and for the Shimmulator in on-telescope, off-sky mode to the right. Note that the cone of rays converging from the secondary is nearly the same in all three cases, as designed.

the whole Shimmulator optics from the $0.594 \mu\text{m}$ laser source off the dummy solid secondary, (shown in Fig. 8) and to the phase-shifting interferometer. Our original interferometric phasemaps had 90–100 waves of aberration. The fringes dance around, with some fringes moving by a couple of fringes at 1–2 Hz. During these initial interferometric tests of the Shimmulator in the Large Polishing Lab at the Steward Observatory Mirror Lab, the polishing station for the Large Binocular Telescope mirror was turned off, so vibrations may have been fortuitously minimal. The air suspension qualitatively improves the fringe stability by a factor of 2–3 in fringe peak-to-peak motion, and by turning the Mirror Lab air conditioner off, we improve the fringe stability by another factor of 2–3. Most of the vibrations are probably coming from the air handlers in the Mirror Lab Casting area.

Since early June, we have modified the CGH source table so that the CGH and the fiber sources can move together as a whole. This made alignment of the CGH-source optical axis to the large optics optical axis *much* easier and less iterative, and allowed us to align the CGH to the fiber sources prior to installation in the Shimmulator tower. We have used these new CGH source adjustments *and* a better focussing of the CGH with respect to the source to ensure that the collimated alignment marks are indeed collimated to obtain a very good a-comatic focus (judged by eye) through all the optics. Unfortunately, the position of the focus was in the middle of the interferometer, 6 inches past the desired and designed position of the focus. We compensated for this focus shift by translating the dummy secondary mirror 1/6-th of an inch up with respect to the large lenses. We have reduced the horrid 90–100 wave aberrations to 10–30 waves of coma by achieving the optomechanical alignment tolerances of the Shimmulator optics independent of feedback from the interferometer. The new adjustments available for the CGH table have helped considerably. Since we were able to eliminate most of these 10–30 waves of coma (down to 4–6 waves of astigmatism and coma) by slightly adjusting the centration of the small doublet, we are confident that we will soon reduce the aberrations to less than a wave with a perfectly mechanically-aligned Shimmulator by fine-tuning the centration of the dummy secondary with the manual hexapod to within $100 \mu\text{m}$. In about a week, after alignment of

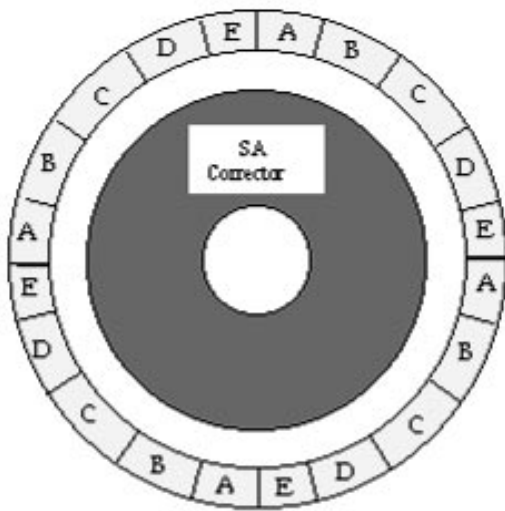


Figure 6. Map of CGH with alignment markings, and a photo of the CGH. The map shows the five sets (A,B,C,D,E) of alignment marks, with four copies of each. Four of these alignment-mark sets bring the light to a focus at four different points along the beam path. One of these alignment marks is a retro-focus on the sources, and the other three alignment marks bring light to a focus on the bottom of the small-doublet, a fold-flat, and the bottom of the second large lens. These CGH alignment foci allow centration and distance-calibration of the different optics and tilt-elimination and focus of the CGH itself with respect to the sources. The fifth alignment mark collimates the light and helps in the CGH focussing. The central pattern of the CGH corrects for the spherical aberrations of the big lenses upstream.

the Shimmulator with the dummy solid secondary, we will add the wavefront sensor camera, the off-axis parabolas, the spinning turbulence plates, and the two imaging cameras to the Top Box, and then full open-loop testing of the Shimmulator will begin.

4. PLANNED TESTING PROGRAM

Our first test will be to measure the mapping error of the Shimmulator optics. We will place a string with regularly spaced fiducials across different diameters of the dummy solid secondary, and then take interferograms with these fiducials, which will show the distortion of the pupil at the secondary by the Shimmulator optics. If the distortion is above 2-3 mm at any one pupil point, we will tune up the distortion by changing the spacing of the small doublet or any of the hexapod 5 degrees of freedom of the solid secondary mirror.

Our second test will be to place a static wavefront of turbulence in the system with the turbulence plates and to measure simultaneously the outputs of the wavefront sensor camera, the phase-shifting interferometer, and the imaging camera. We can then check these measurements for self-consistency and also to test sensor performance. We will repeat these comparisons for many different static wavefronts.

Our third test will be to measure and analyze the output of the wavefront sensor camera with spinning turbulence plates. This test will provide signal-to-noise information of the wavefront sensor in the Shimmulator, and will quantify the dynamical characteristics of the turbulence plates, though much of this information will have already been obtained with an independent benchtop AO system.⁵

All three of the above tests should be completed in August. In September, we expect delivery of the full adaptive secondary (with spherical thin mirror) from electromechanical integration in Italy. We will first check the electrical and computer interfaces, and then install the adaptive secondary in the Shimmulator. The actuators of the adaptive secondary will be adjusted to minimize the aberration without turbulence. This will be the first time the adaptive secondary will be tested optically and in an inverted orientation, so these turbulence-free actuator positions will become the nominal actuator home positions. Interferometric gap sensors¹⁵ built into the adaptive secondary will

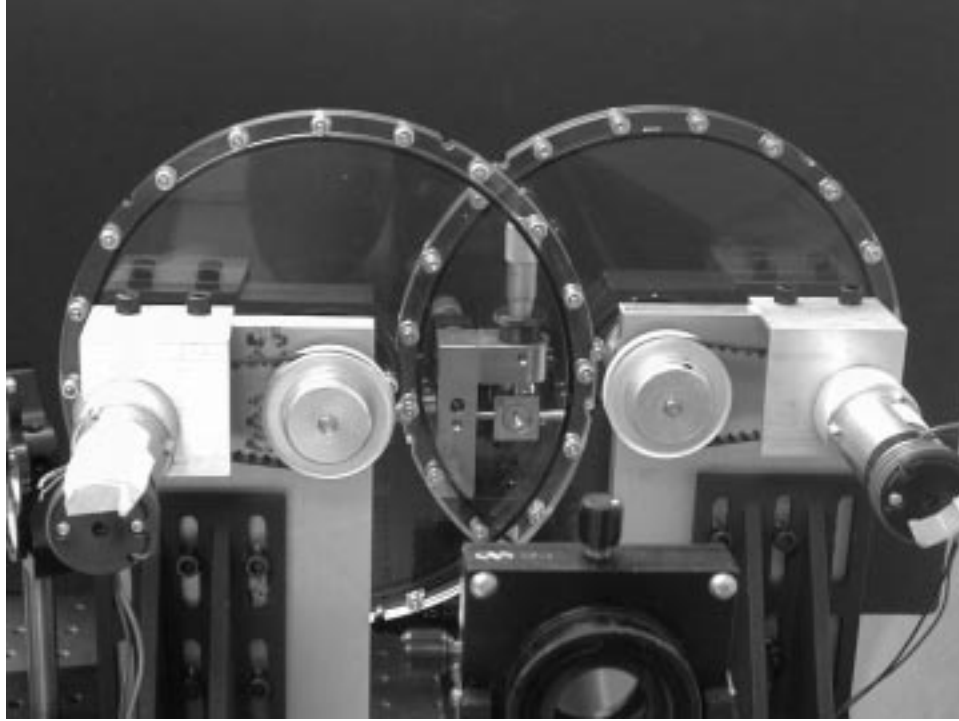


Figure 7. Two turbulence plates attached to the motors which will spin them. Note the pinhole source in the background, and the collimating lens in the foreground.

serve to periodically calibrate the real-time capacitive gap sensors, and will also be used to help us tune the actuators to give the right spherical shape on the secondary mirror.

Our fourth test in the Shimmulator (this time with adaptive secondary) will be to close-the-loop without turbulence. This means that we start with the actuators away from their home positions, and then turn the whole adaptive optics system on (WFS, wavefront computer, and adaptive secondary) so that the system determines the home positions of the actuators from scratch.

Our fifth test will be to close the loop in the Shimmulator with static turbulence, and simultaneously measure performance of all the sensors. This will tell us the details of the fitting error and reconstructor error limitations of the MMT AO system.

Our sixth test will be to close the loop on the adaptive secondary in the presence of dynamic turbulence of varying speeds, spatial coherence lengths, and varying laser source intensities. This will tell us how well our adaptive secondary AO system has been built to match specifications, and whether we can proceed soon thereafter to the telescope.

Once these tests are satisfactorily completed (hopefully by December 1999), we will replace the spherical shell in the secondary with the true hyperboloid aspherical shell, and repeat tests 4–6. This should be much quicker than with the spherical shell. Then the whole AO system will be taken to the telescope site on Mt. Hopkins, where we will repeat these Shimmulator tests in an off-telescope tower and also in the on-telescope, off-sky configuration (see Fig. 5). Finally, first light for MMT natural guidestar AO should be in early 2000, soon to be followed by laser guidestar first light. Despite the relative complexity of the adaptive secondary, this first light should be relatively seamless due to the extensive off-telescope testing, and significant contributions to high-resolution-imaging infrared astronomy should be commonplace from the MMT in 2000 and beyond.

ACKNOWLEDGMENTS

Manny Montoya, Rich Gonzalez, Curt Blair, Hanna Coy, Jeff Capara, Buddy Powell, Jim Harrington, Ann Bauer, John Kapp, Roger Ceragioli, Steve Warner, Chris Stetson and Bryan Smith have provided valuable assistance for the



Figure 8. Installation of the solid dummy secondary above the two large lenses into the top part of the Shimmulator tower. The top part of the tower was then hoisted by crane to be secured atop the bottom section of the tower.

MMT AO project. Brian McLeod asked “How are you going to test the secondary?” at just the right time, and also searched the CfA library for precise atomic physics information on the yellow HeNe transition. Troy Rhoadarmer helped to build and test the WFS & turbulence plates, described in part here, and his work on the T37 benchtop AO system served as a model upon which much of the test-plan for the Shimmulator was developed. Troy also reviewed this paper. We have been supported by the Air Force Office of Scientific Research under grant #F49620-94-1-0437 and grant #F49620-96-1-0366.

REFERENCES

1. G. Brusa, A. Riccardi, V. Biliotti, C. DelVecchio, P. Salinari, P. Stefanini, P. Mantegazza, R. Biasi, C. Franchini, and D. Gallieni, “The adaptive secondary mirror for the 6.5 conversion of the Multiple Mirror Telescope: first laboratory testing results,” *Proc. SPIE* **3762**, 1999.
2. R. J. Sarlot and J. H. Burge, “Optical system for closed-loop testing of the adaptive optic convex mirror,” *Proc. SPIE* **3430**, p. 126, 1998.
3. G. Brusa, A. Riccardi, S. Ragland, S. Esposito, C. DelVecchio, L. Fini, P. Stefanini, V. Biliotti, P. Ranfagni, P. Salinari, D. Gallieni, R. Biasi, P. Mantegazza, G. Sciocco, G. Noviello, and S. Invernizzi, “Adaptive secondary P30 prototype: laboratory results,” *Proc. SPIE* **3353**, p. 764, 1998.
4. P. C. McGuire, T. A. Rhoadarmer, M. Lloyd-Hart, J. C. Shelton, J. R. P. Angel, G. Z. Angeli, J. M. Hughes, B. C. Fitz-Patrick, M. L. Rademacher, P. Schaller, M. A. Kenworthy, F. P. Wildi, J. G. Capara, M. P. Lesser, and D. B. Ouellette, “Construction and testing of the wavefront sensor camera for the new MMT adaptive optics system,” *Proc. SPIE* **3762**, 1999.
5. T. A. Rhoadarmer, P. C. McGuire, J. M. Hughes, M. Lloyd-Hart, J. R. P. Angel, S. Schaller, and M. A. Kenworthy, “Laboratory adaptive optics system for testing the wavefront sensor for the new MMT,” *Proc. SPIE* **3762**, 1999.
6. D. W. McCarthy, J. H. Burge, J. R. P. Angel, J. Ge, R. J. Sarlot, B. C. Fitz-Patrick, and J. L. Hinz, “ARIES: Arizona infrared imager and echelle spectrograph,” *Proc. SPIE* **3354**, p. 750, 1998.

7. M. Lloyd-Hart, "Thermal performance enhancement of adaptive optics by use of a deformable secondary mirror," *submitted to PASP* , 1999.
8. D. M. Williams, C. L. Thompson, G. H. Rieke, and E. F. Montgomery, "Compact high-resolution IR spectrometer for the Columbus Telescope," *Proc. SPIE* **1946**, p. 482, 1993.
9. W. F. Hoffmann, G. G. Fazio, K. Shivanandan, J. L. Hora, and L. K. Deutsch, "MIRAC: a mid-infrared array camera for astronomy," *Proc. SPIE* **1946**, p. 449, 1993.
10. T. A. Rhoadarmer, *Construction and Testing of Components for the 6.5 m MMT Adaptive Optics System*. PhD thesis, University of Arizona, Optical Sciences Center, 1999.
11. T. A. Rhoadarmer, J. R. P. Angel, S. M. Ebstein, M. Lloyd-Hart, M. A. Kenworthy, I. Lanum, M. L. Rademacher, B. C. Fitz-Patrick, and P. C. McGuire, "Design, construction, and testing of a low-cost, broadband static phase plate for generating Kolmogorov turbulence," (*to be published*) , 1999.
12. C. Zhao, "Description of the AO interferometer," *U.Arizona/Steward Observatory internal document* , (May 1999).
13. B. L. Stamper, "Shimmulator interferometer laser source for the Multiple Mirror Telescope upgrade," *U.Arizona/Steward Observatory internal document* , (June 1999).
14. J. C. Shelton, M. Lloyd-Hart, J. R. P. Angel, and D. G. Sandler, "The 6.5m MMT laser-guided adaptive optics system: Overview and progress report II," *Proc. SPIE* **3126**, p. 2, 1997.
15. R. L. Johnson, J. R. P. Angel, M. Lloyd-Hart, and G. Z. Angeli, "Miniature instrument for the measurement of gap thickness using poly-chromatic interferometry," *Proc. SPIE* **3762**.